

# Ultrafast opto-terahertz photonic crystal modulator

L. Fekete, F. Kadlec, and P. Kužel

*Institute of Physics, Academy of Sciences of the Czech Republic, Na Slovance 2, 182 21 Prague 8, Czech Republic*

H. Němec

*Chemical Center, Lund University, Getingevägen 60, 222 41 Lund, Sweden*

Received November 28, 2006; accepted December 22, 2006;  
posted January 4, 2007 (Doc. ID 77557); published February 15, 2007

We present an agile optically controlled switch or modulator of terahertz (THz) radiation. The element is based on a one-dimensional photonic crystal with a GaAs wafer inserted in the middle as a defect layer. The THz electric field is enhanced in the photonic structure at the surfaces of the GaAs wafer. Excitation of the front GaAs surface by ultrashort 810 nm laser pulses then leads to an efficient modulation of the THz beam even at low photocarrier concentrations ( $\approx 10^{16} \text{ cm}^{-3}$ ). The response time of the element to pulsed photoexcitation is about 130 ps. © 2007 Optical Society of America

OCIS codes: 160.5140, 300.6270, 300.6530, 230.1150, 230.4110.

The generation and control of pulsed and continuous-wave terahertz (THz) radiation has received considerable attention during the past years.<sup>1,2</sup> As future short-range indoor communication systems may be designed for the sub-THz or THz range, one can expect a growing research emphasis put on the manipulation of both guided and freely propagating THz beams by means of agile switches, modulators, and phase shifters controlled either optically or electronically. Quasi-optical devices allowing fast transfer of information from the optical to the THz spectral band are of particular interest.

High-resistivity semiconductors show big potential for the optical control of their reflectance or transmittance in the gigahertz (GHz) and THz spectral ranges.<sup>3–7</sup> They are transparent in their ground state, whereas the photoexcitation of electrons leads to a marked increase in the absorption coefficient in the THz range. This enables setting up relatively simple elements in which the propagation of THz waves is controlled by visible light.

An important parameter that deserves consideration is the lifetime of free carriers in the semiconductor. A short—subnanosecond or picosecond—lifetime allows a high switching rate,<sup>4</sup> while semiconductors with a long free-carrier lifetime can be used as optically controlled attenuators.<sup>8</sup> In the latter case, the slow response allows one to reduce considerably the optical pump intensity needed for an appreciable modulation of the THz beam, because the photocarrier density is proportional to the lifetime under continuous illumination.

We have recently reported a broadband ultrafast opto-THz switch based on a thick GaAs wafer<sup>7</sup> that allows one to modulate its THz reflectivity between the antireflective and highly reflective limits by varying the photoexcitation intensity. Its drawback is a relatively high carrier concentration required for efficient switching in the THz range. In this Letter we report on an agile optical THz modulator consisting of a thin GaAs platelet enclosed in a one-dimensional photonic crystal (PC) structure. As the investigated

structure has a resonant character, it shows a narrower operation bandwidth and is suitable for applications with quasi-monochromatic THz radiation. At the same time, owing to the THz electromagnetic field enhancement in the GaAs layer, this device allows us to efficiently modulate the THz light at substantially lower photoexcitation fluences, while the speed of the switching is determined by the lifetime of the carriers at the surface of the GaAs wafer.

The experiments were performed with a PC structure composed of a multilayer stack of wafers—(0001) oriented crystalline quartz (with THz refractive index  $n_L=2.10$  and thickness  $d_L=60\pm 1 \mu\text{m}$ ) and (001) oriented MgO (refractive index  $n_H=3.12$ , thickness  $d_H=42\pm 1 \mu\text{m}$ ) as low- and high-index materials. The central MgO layer was replaced by a GaAs platelet ( $n_D=3.55$ ,  $d_D=65\pm 1 \mu\text{m}$ ) acting as a defect. The sequence of the layers, all with a square shape of  $7 \text{ mm} \times 7 \text{ mm}$ , reads as (LH)<sup>4</sup>LDL(HL)<sup>4</sup>. The whole structure was assembled into a holder with a 4 mm clear aperture.

This device can be described as a Fabry–Perot interferometer with two Bragg mirrors enclosing a thin cavity made of GaAs in the middle.<sup>9–11</sup> The THz spectrum of such a structure exhibits forbidden bands where the transmission is inhibited (or significantly reduced) and so-called defect modes inside those bands, which are characterized by a high transmission coefficient. Our Bragg mirrors were composed of typical quarter-wave stacks: the central wavelength of the lowest forbidden band is equal to  $2d_{\text{tot}}$ , where  $d_{\text{tot}}$  is the optical thickness of the unit cell ( $d_{\text{tot}}=n_H d_H+n_L d_L$ , and  $n_H d_H \approx n_L d_L$ ). The device operates at frequency  $f_0$  corresponding to that of the defect mode in the lowest forbidden band.

MgO and SiO<sub>2</sub> are transparent for both optical and THz radiation: the optical pump thus creates free carriers at the surface of the central GaAs wafer. They induce losses in the structure in the THz range and temporarily inhibit its THz transmittance. Since the defect layer is approximately a half-wave plate,

i.e.,  $n_D d_D \approx d_{\text{tot}}$ , the defect mode is located near the center of the forbidden band. It follows from the analysis shown in Ref. 9 that if the low refractive index layer is adjacent to the defect, the defect mode has odd symmetry. Consequently, the electric field of the standing waves inside the structure exhibits antinodes at the defect surfaces. This wave profile enables a strong interaction of the THz radiation with photocarriers and is suitable for efficient THz light modulation.

The time response of the structure essentially depends on the lifetime  $\tau_c$  of free carriers in GaAs (which is about 110 ps for our sample<sup>12</sup>) and on the lifetime  $\tau_{\text{PC}}$  of the THz wave at  $f_0$  in the PC [ $\tau_{\text{PC}} = 1/(\pi\Delta f)$ ]. Here  $\Delta f$  stands for the full width at half-maximum (FWHM) of the defect mode in the power transmittance. The time response of the PC is controlled solely by the carrier lifetime if  $\tau_c \gg \tau_{\text{PC}}$ ; otherwise, the switching is slowed down due to the response of the PC. A more elaborate analysis of the time response of the modulator is beyond the scope of the present Letter.

The experiments were realized by using the time-domain THz spectroscopy with a femtosecond Ti:sapphire amplified laser source. The pulse train was split into three branches—one used for photoexcitation, one for the generation of the THz pulses via optical rectification, and one for electro-optic sampling of the THz radiation.<sup>12</sup> The sample was held in the focus of the THz beam with a diameter of 2.8 mm for frequencies close to 600 GHz. The pump beam was spatially expanded to improve the excitation homogeneity across the 4 mm aperture of the sample. The incident pump fluence was varied between 0.4 and  $26 \mu\text{J}/\text{cm}^2$  by using neutral-density filters and was carefully measured by using another empty 4 mm aperture positioned exactly at the sample place.

Figure 1 shows examples of time-domain THz waveforms. The scans were typically 200 ps long to achieve a spectral resolution of 5 GHz. The complex transmission spectra (see examples in Fig. 2) were calculated from the Fourier transformation of the time-domain data. The spectrum of the reference waveform  $E_{\text{ref}}$ , obtained in an experiment when the PC was removed from the THz beam path, is used for the normalization of all the transmission spectra. The data were first measured with the pump beam off to determine the steady-state characteristics  $E_0(t)$  of the PC. The ground state transmittance corresponds to curve (a) in Fig. 2. In the experiments with the pump beam on, our setup<sup>12</sup> allowed us to measure the photoinduced change, the so-called transient waveform  $\Delta E(t)$  [see Fig. 1(c)], with a high sensitivity. The actual waveform transmitted through the photoexcited sample is then  $E = E_0 + \Delta E$ . Note that the transient waveform obtained for a low pump fluence shows a slowly damped quasi-monochromatic character related to the fact that the photocarriers strongly decrease the transmission of the PC at the defect frequency while the transmission is only weakly influenced at other frequencies [see curves (a) and (b) in Fig. 2]. In the high-pump-fluence limit [curve (c) in Fig. 2] the defect mode is entirely sup-

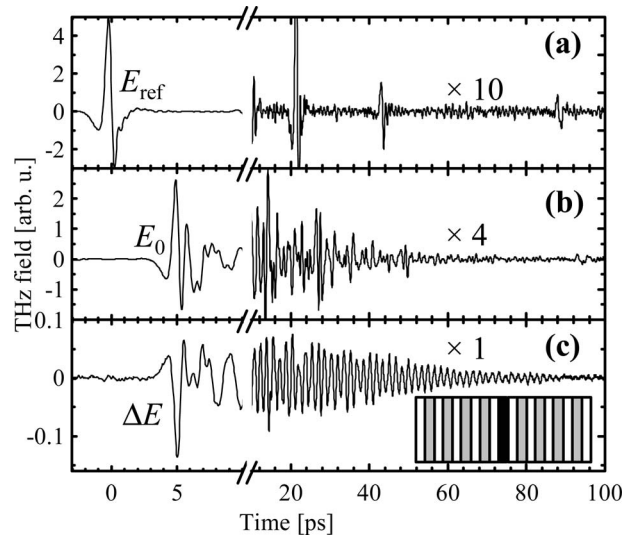


Fig. 1. Examples of THz waveforms. (a) Reference waveform measured without PC. (Features at 10, 21, 43, and 88 ps are due to reflections on various elements in the THz beam path; the long-lasting irregular signal is related to residual water vapor.) (b) Waveform transmitted through the PC in the ground state. (c) Transient waveform obtained at  $0.8 \mu\text{J}/\text{cm}^2$  pump fluence. Inset, scheme of the structure (white,  $\text{SiO}_2$ ; gray,  $\text{MgO}$ ; black, GaAs).

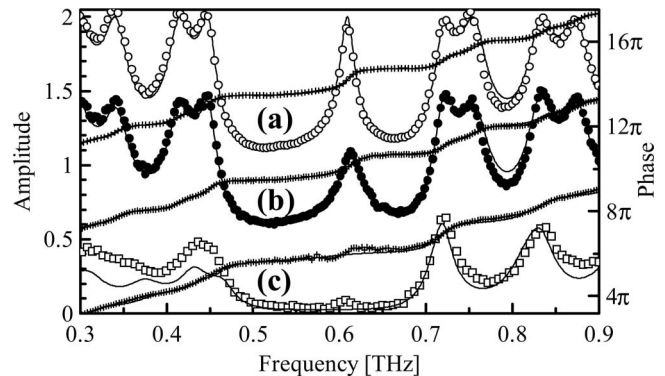


Fig. 2. Complex transmittance of the PC structure as a function of the pump pulse fluence: (a)  $0 \mu\text{J}/\text{cm}^2$  (ground state), (b)  $0.8 \mu\text{J}/\text{cm}^2$ , (c)  $26 \mu\text{J}/\text{cm}^2$ . The pump-probe delay is 5 ps. Symbols, experimental data; lines, calculation by using transfer matrix formalism. Vertical offsets of 1 ( $8\pi$ ) and 0.5 ( $4\pi$ ) are applied to the amplitude (phase) of the data corresponding to curves (a) and (b), respectively.

pressed, but the band structure at other frequencies is also strongly distorted.

The theoretical investigation of the structure was performed by using the transfer matrix formalism.<sup>13</sup> The calculated steady-state spectrum fits the measured data quite well; we obtain an excellent match of the frequency of the defect mode and of the forbidden band edges if we slightly adjust the nominal thicknesses of  $\text{MgO}$  and GaAs wafers: we used  $d_H = 42.7 \mu\text{m}$  and  $d_D = 64.5 \mu\text{m}$  as best-matching values. The defect mode frequency then amounts to  $f_0 = 609 \text{ GHz}$ , in agreement with the experiment; its FWHM is  $\Delta f = 16.7 \text{ GHz}$ .

Concerning the simulation of the photoexcited PC, a linear absorption process of the pump beam in

GaAs was assumed (with absorption coefficient  $\alpha = 1.3 \mu\text{m}^{-1}$ ). Using the transfer matrix formalism, we calculated the absorbed optical pump intensity in GaAs near 810 nm to be 75% of the measured intensity incident on the PC. From this value we can estimate the surface density of free carriers for any pump fluence; the complex THz refractive index of photoexcited GaAs is then evaluated by using the Drude model.<sup>14</sup> The experimental spectra match very well the theoretical ones for all the pump fluences (see Fig. 2) provided that the surface density of free carriers estimated from the experimental conditions is systematically divided by a factor of 1.5. This small discrepancy can be explained by optical power losses due to interferences in micrometer sized air cavities between the constituent layers of the PC and by a small error in the calibration of the powermeter used to estimate the pump fluence. After this correction we obtain a carrier density of  $10^{16} \text{cm}^{-3}$  for the lowest fluence used ( $0.4 \mu\text{J}/\text{cm}^2$ ).

Power modulation spectra, defined as the ratio of the power transmittance of the PC in the excited and ground states, are shown in Fig. 3. Note that the modulation occurs mainly in the vicinity of the defect mode and that nearly 50% modulation of the transmitted power is obtained for the free-carrier concentration of  $1 \times 10^{16} \text{cm}^{-3}$ . Let us estimate now what minimum pulse energy is required for achieving 50% modulation under optimal conditions. In principle, the THz radiation at 600 GHz (i.e., at a 0.5 mm wavelength) can be focused more tightly than it was in our experiment. For example, for a 600 GHz Gaussian beam with a waist diameter of 2 mm in a quartz the confocal beam parameter<sup>15</sup> exceeds  $z_0 \geq 12 \text{mm}$ , which is more than the length corresponding to the lifetime of the THz wave at 600 GHz in our

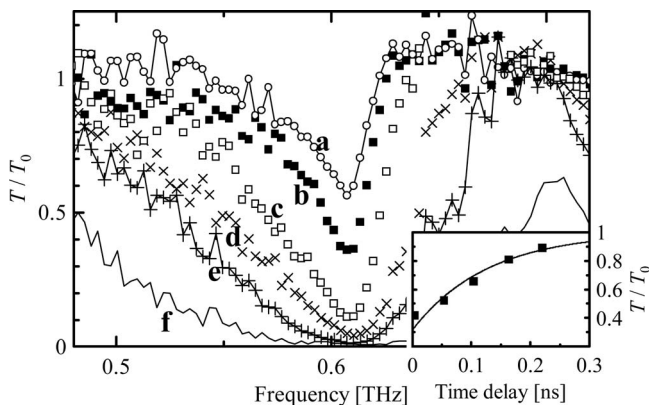


Fig. 3. Ratio between the power transmission spectra of the PC in photoexcited and ground state  $T/T_0$  near the defect mode. Pump pulse fluences ( $\mu\text{J}/\text{cm}^2$ ) and free-carrier densities ( $10^{16} \text{cm}^{-3}$ ): (a) 0.4, 1.0; (b) 0.8, 2.0; (c) 2.4, 6.1; (d) 5.3, 13.5; (e) 8.0, 20; (f) 26, 66. Pump-probe delay, 5 ps. Inset, decay of the relative power transmission at 609 GHz for  $0.8 \mu\text{J}/\text{cm}^2$  versus pump-probe delay time.

PC:  $c/(\pi\Delta f) \approx 6 \text{mm}$ . The THz capabilities of the structure then should not be significantly reduced if an input aperture of 2 mm is used with appropriate focusing THz optics. In this case the incident pulse energy of 10 nJ (currently available from common femtosecond Ti:sapphire oscillators) would be sufficient to induce a 50% modulation of the THz light.

The decay of the THz modulation in time is obtained if the measurements are performed as a function of the pump-probe delay. Results of this experiment along with an exponential fit are shown in the inset of Fig. 3. The time constant of the decay is  $128 \pm 12 \text{ps}$ , which is in a good agreement with the carrier lifetime in the GaAs wafer.

In summary, we have demonstrated the possibility of ultrafast ( $\sim 100 \text{ps}$ ) modulation of THz radiation controlled by optical pulses by using a one-dimensional photonic crystal with a GaAs defect. Our results indicate that 50% modulation may be possible with a pump pulse energy of the order of 10 nJ, which can be provided by commercial femtosecond Ti:sapphire oscillators.

Financial support by the Academy of Sciences of the Czech Republic (project 1ET300100401) and by its Grant Agency (project KJB100100512) is acknowledged. P. Kužel's e-mail address is kuzelp@fzu.cz.

## References

1. B. Ferguson and X.-C. Zhang, *Nat. Mater.* **1**, 26 (2002).
2. H. K. Choi, *Long-Wavelength Infrared Semiconductor Lasers* (Wiley, 2004).
3. J. Bae, H. Mazaki, T. Fujii, and K. Mizuno, in *1996 IEEE MTT-S International Microwave Symposium Digest* (IEEE, 1996), Vol. 3, p. 1239.
4. T. Nozokido, H. Minamide, and K. Mizuno, *Electron. Commun. Jpn., Part 2: Electron.* **80**, 1 (1997).
5. S. Lee, Y. Kuga, and R. A. Mullen, *Microwave Opt. Technol. Lett.* **27**, 9 (2000).
6. A. Chelnokov, S. Rowson, J.-M. Lourtioz, L. Duvillaret, and J.-L. Coutaz, *Electron. Lett.* **34**, 1965 (1998).
7. L. Fekete, J. Y. Hlinka, F. Kadlec, P. Kužel, and P. Mounaix, *Opt. Lett.* **30**, 1992 (2005).
8. S. Biber, D. Schneiderbanger, and L.-P. Schmidt, *Frequenz* **59**, 141 (2005).
9. H. Němec, L. Duvillaret, F. Quemeneur, and P. Kužel, *J. Opt. Soc. Am. B* **21**, 548 (2004).
10. H. Němec, P. Kužel, F. Garet, and L. Duvillaret, *Appl. Opt.* **43**, 1965 (2004).
11. H. Němec, P. Kužel, L. Duvillaret, A. Pashkin, M. Dressel, and M. Sebastian, *Opt. Lett.* **30**, 549 (2005).
12. H. Němec, F. Kadlec, C. Kadlec, P. Kužel, and P. Jungwirth, *J. Chem. Phys.* **122**, 104504 (2005).
13. R. Jacobsson, in *Progress in Optics*, E. Wolf, ed. (North-Holland, 1965), Vol. 5, Chap. 5.
14. N. W. Ashcroft and N. D. Mermin, *Solid State Physics* (Holt, Rinehart and Winston, 1976).
15. A. Yariv and P. Yeh, *Optical Waves in Crystals* (Wiley, 1984).